Understanding the Origins of Nucleophilic Hydride Reactivity of Sodium Hydride-Iodide Composite

Zonghan Hong,[a] Derek Yiren Ong,[a] Subas Kumar Muduli,[a,b] Pei Chui Too,[a] Guo Hao Chan,[a] Ya Lin Tnay,[a] Shunsuke Chiba,*[a] Yusuke Nishiyama,*[c] Hajime Hirao,*[a] and Han Sen Soo*[a,d,e]

Abstract: Sodium hydride (NaH) has been commonly used as a Brønsted base in chemical syntheses, while it has rarely been employed to add hydride (H^-) to unsaturated electrophiles. We previously developed a procedure to activate NaH through the addition of a soluble iodide source and found that the new NaH-NaI composite can effect even stereoselective nucleophilic hydride reductions of nitriles, imines, and carbonyl compounds. In this work, we report that mixing NaH with NaI or LiI in tetrahydrofuran (THF) as a solvent provides a new inorganic composite, which consists of NaI interspersed with activated NaH, as revealed by powder X-ray diffraction, and both solid-state nuclear magnetic resonance and X-ray photoelectron spectroscopy. DFT calculations implicate that this remarkably simple inorganic composite, which is comprised of NaH and NaI, gains nucleophilic hydridic character similar to covalent hydrides, resulting in unprecedented and unique hydride donor chemical reactivity.

Introduction

Sodium hydride (NaH) is one of the simplest known ionic compounds with a cubic halite crystal structure. Similar to other alkali metal hydrides that consist of M^+ (M = alkali metal) and H^- ions bound together strongly via electrostatic attraction, NaH is practically insoluble in organic solvents and reacts with protic solvents.[1] Consequently, the reactivity of NaH was previously thought to be limited exclusively to Brønsted basic or single electron transfer (SET) activity,[1] and has rarely been invoked as a two-electron hydride (H^-) transfer agent.[2] Instead, a number of covalent hydrides, including boranes, silanes, metal borohydrides, and metal aluminum hydrides have typically been utilized as the reagents of choice in nucleophilic H^- transfer reactions.[3]

Our team has been independently working on developing new reaction designs for synthetic organic chemistry[4] with Earth-abundant reagents and also sustainable applications in energy-related research such as artificial photosynthesis.[5] We recently discovered a remarkable and unprecedented decyanation reaction enabled by NaH in the presence of iodide addtiives (Scheme 1).[6] Sodium iodide (NaI), lithium iodide (LiI), and magnesium iodide (MgI_2) were identified as suitable additives for mediating this unusual reaction, implicating the critical role of dissolved iodide in the mixture.[6a] The substrate scope is broad and the stereo-configuration during the nitrile substitution with hydride was retained (Scheme 1).[6a] We have expanded the substrate scope to include other unsaturated compounds such as amides, imines (Scheme 1), esters, and carbonyl compounds.[6a]

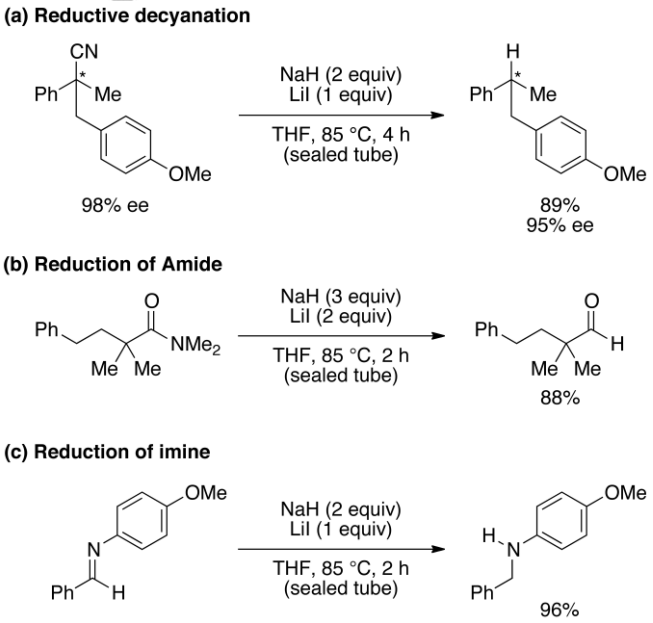

Scheme 1. (a) Nucleophilic hydride substitution of nitrile with retention of stereo-configuration; (b) reduction of amides; and (c) reduction of imines.

Through a series of kinetics experiments, substrate screening, and DFT calculations, we proposed that NaH and the dissolved I^- ions recrystallized as smaller fragments of a NaH-NaI composite.[6a] This composite possesses nucleophilic hydride transfer reactivity, which can potentially be employed in the reduction of numerous unsaturated substrates such as

[a] Z. Hong, D. Y. Ong, Dr. S. K. Muduli, Dr. P. C. Too, G. H. Chan, Dr. Y. L. Tnay, Prof. H. Hirao, Prof. H. S. Soo, Prof. S. Chiba
Division of Chemistry and Biological Chemistry, School of Physical and Mathematical Sciences
Nanyang Technological University, 21 Nanyang Link, Singapore 637371, Singapore
E-mail: yunishiy@jeol.co.jp, hansen@ntu.edu.sg, Shunsuke@ntu.edu.sg
[b] Dr. S. K. Muduli
Energy Research Institute@NTU
Nanyang Technological University, Research Techno Plaza, Singapore 637553, Singapore
[c] Dr. Y. Nishiyama
RIKEN CLST-JEOL collaboration center, Yokohama, Kanagawa 230-0045, Japan;
JEOL RESONANCE Inc. Akishima, Tokyo 196-8558, Japan
[d] Prof. H. S. Soo
Solar Fuels Laboratory
Nanyang Technological University, 50 Nanyang Avenue, Singapore 637553, Singapore
[e] Prof. H. S. Soo
Singapore-Berkeley Research Initiative for Sustainable Energy (SinBeRISE)
1 Create Way, Singapore 138602, Singapore

Supporting information for this article is available on the WWW under

carbonitriles, imines, and carbonyl compounds.[2-3, 7] Given the extensive applicability of this new material, and the plausible use of I^- to activate other simple ionic materials for novel organic transformations, our team has conducted a series of characterization experiments on this NaH-NaI composite. Herein, we present evidence to establish the interfacial interactions between NaH and NaI, which supports our previous experimental and DFT work that the NaH-NaI composite consists of smaller, activated fragments of NaH.

Results and Discussion

Materials Characterization of NaH-LiI and NaH-NaI Composites

In our reactivity and kinetics studies, the decyanation reactions by NaH-LiI and NaH-NaI exhibited an induction period of at least 0.5 h, independent of the substrates. Indeed, the NaH-Na(Li)I composite materials isolated after the thermal treatment in THF could initiate the decyanation reactions without the induction period. These observations suggest that the reaction of NaH with LiI (or NaI) resulted in the formation of new inorganic composite materials that display the remarkable hydride transfer reactivity. Thus, we subjected these composites to a suite of spectroscopic and structural analyses to elucidate the origin of the observed reactivity: powder X-ray diffraction (pXRD), FT-IR spectroscopy, and solid-state NMR spectroscopy provided information about the bulk composition, whereas X-ray photoelectron spectroscopy (XPS) to investigate the surface properties confirmed our previous DFT studies.

The pXRD patterns of the NaI and LiI composites unambiguously demonstrated that in the *bulk composition* for *both* of the materials, *the same cubic NaI crystal phase* was present in crystalline form, and there was remarkably *no* trace of LiI (Figure 1).[8] Appreciable amounts of NaH were observed in both of the samples prepared from NaI or LiI, which confirmed that the NaH coexists with the NaI crystal phase.[9] No peaks corresponding to NaOH or LiOH were observed, indicating that the composites did not contain *crystalline* components of both hydroxides. Rietveld refinement performed on the pXRD data suggested that the NaH-LiI sample had a composition of $NaI_{0.73}H_{0.27}$ (Figure 1a) whereas the NaH-NaI composite had a composition of $NaI_{0.63}H_{0.37}$ (Figure 1b).[8c, 9] After using the NaH-NaI composite for the decyanation, the composition was converted into $NaI_{0.81}H_{0.19}$ (see the Supporting Information, Figure S1a and Table S1). The pXRD studies provide evidence that LiI had dissolved and recrystallized as NaI through solvothermal salt metathesis,[10] and some crystalline domains of NaH remained in the bulk composition of both samples.

To probe the *surface* content of the composite materials, XPS was conducted on the composites (Figures 2 and S2) as well as pristine samples of NaH, NaI, and LiI (Figures S3-S5 respectively, and Table S2). All the XPS data have been calibrated internally to the C *1s* signal from the carbon tape used. Remarkably, for the NaH-LiI composite, a minor component (26%) is observed at 1072.0 eV (Figure 2a), which does not correspond to the Na *1s* peaks of pristine NaH or NaI (Figure S3a and S4a, respectively) that coincide around 1070 eV.[11] Likewise, for the NaH-NaI composite, a new appreciable component (44%) is detected at 1072.4 eV (green line, Figure S2a), which is distinct from the Na *1s* signals at 1069.8 eV for NaH and NaI (Figure S3a and S4a, respectively).

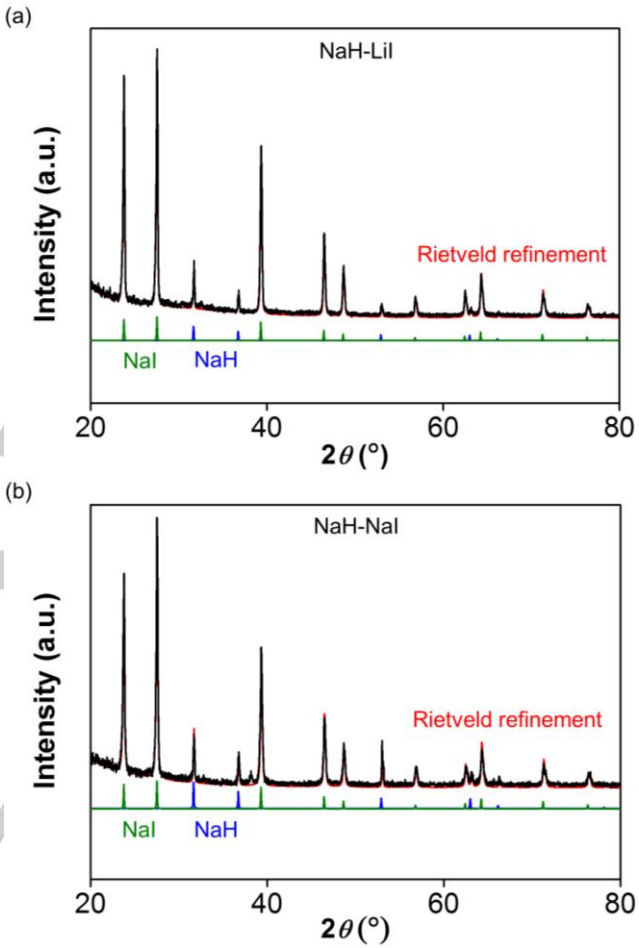

Figure 1. Powder X-ray diffraction study for (a) the NaH-LiI sample, and (b) the NaH-NaI sample. The experimental data (black) and the Rietveld refinements (red) are compared to the components of NaI (green) and NaH (blue).

More intriguingly, the I $3d_{5/2}$ and $3d_{3/2}$ bands of the NaH-LiI XPS spectrum also appear to consist of two components, one of which is the expected peak for NaI at 618.6 and 629.9 eV (42%), while the other component at 620.3 and 631.6 eV (58%) suggests some unique, higher energy photoemission distinct from a typical monoanionic iodide (Figure 2b).[11] The NaH-NaI sample exhibits behavior similar to that of NaH-LiI, with NaI as the minor component (31%) at 618.6 and 630.0 eV, and a new major component at 620.7 and 632.2 eV (green line, Figure S2b) is attributable to the unique NaH-NaI composite.[11b] No significant amounts of Li were detected by XPS measurements. Due to the presence of O *1s* signals arising from the acrylate

adhesive in the carbon tape, we could not obtain conclusive information about the absence of amorphous forms of NaOH or LiOH.

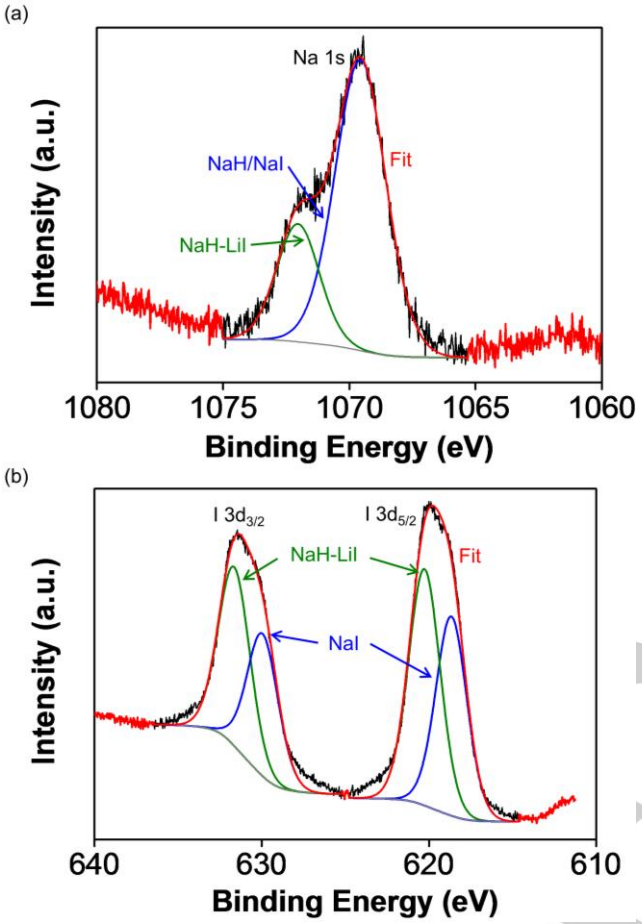

Figure 2. (a) Na 1s XPS data for the NaH-LiI composite (black) with the fit (red) and the components attributable to NaH or NaI (blue), and the new component arising from interaction between NaH and NaI (green). (b) I *3d* XPS data for the NaH-LiI composite (black) with the fit (red) and the components attributable to NaI (blue), and the new component arising from interaction between NaH and NaI (green).

Attenuated total reflectance Fourier transform infrared (ATR-FTIR) spectroscopy was undertaken on the composites, but no distinctive band was observed in the mid-IR region, as expected for NaH.[12] However, after the NaH-NaI sample had been employed for a reduction reaction, the ATR-FTIR spectrum revealed the presence of CN^- (2086 cm^{-1}) in the bulk material as anticipated.[6a]

We performed a set of solid-state ^{7}Li, ^{23}Na, and ^{127}I NMR measurements to understand the structures of the NaH-NaI and NaH-LiI composites. We have also measured the NMR spectra of NaH, NaI, and LiI as references. The peak positions in the NMR spectra are very sensitive to the local environment of each nucleus. Thus, if two samples show NMR spectra with the peaks at the same positions, we can safely conclude that the local structures around the observed nuclei are very similar to each other. As shown in Figure 3, the ^{127}I NMR spectra of the NaI, NaH-NaI, and NaH-LiI samples gave sharp peaks at 177 ppm, which differ significantly from that of LiI (358 ppm). This result clearly shows the remarkable absence of the LiI structure in the NaH-LiI composite. The data also strongly indicates that the local environments of ^{127}I are almost the same in the detectable *bulk* environments of the NaI, NaH-NaI, and NaH-LiI samples, suggesting the retention and formation of the cubic NaI structure in both the NaH-NaI and NaH-LiI composites, respectively. The sharp lineshapes of ^{127}I NMR spectra indicate the absence of quadrupolar coupling, suggesting that the cubic symmetry in the crystals remains. This agrees with the pXRD observations as well. The ^{127}I NMR lineshape also does not change in the absence and presence of ^{1}H decoupling (Figure S6). These data show that the^{127}I nuclei are located at greater than several Å away from ^{1}H in the NaH-LiI and NaH-NaI samples.

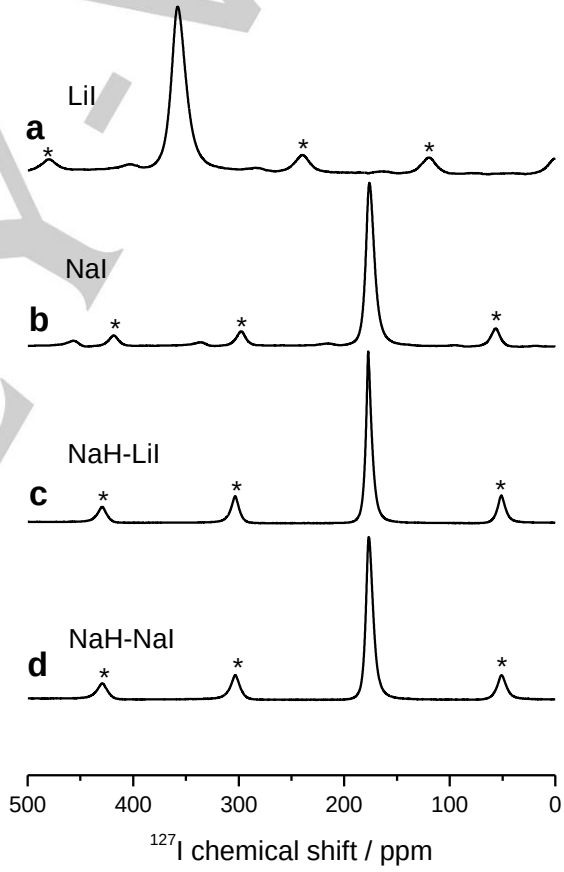

Figure 3. ^{127}I NMR spectra of (a) LiI; (b) NaI; (c) NaH-LiI composite; (d) NaH-NaI composite. The spinning sidebands signals are marked with asterisks.

Figure 4 illustrates the ^{7}Li NMR spectra of LiI, LiH, and NaH-LiI composite. The ^{1}H decoupled ^{7}Li NMR spectrum of NaH-LiI composite is also shown. All the lineshapes are rather sharp, but due to the small quadrupolar moments in ^{7}Li, it is inconclusive to be more definitive about the local symmetry in ^{7}Li based on the

lineshapes. Although all the spectra were very similar, closer inspection shows a small difference in the chemical shifts. While LiH (Figure 4b) and the NaH-LiI (Figure 4c) composition give identical peak positions, the LiI sample (Figure 4a) gives a slight shift toward the high-frequency side. This suggests that the ^{7}Li environment of the NaH-LiI composite is closer to the structure of LiH, rather than that of LiI. The absence of LiI in the NaH-LiI sample agrees with ^{127}I NMR and pXRD observations. The ^{1}H decoupling improves the resolution in the NaH-LiI spectrum (Figure 4c). This clearly demonstrates the presence of proximity between ^{1}H and ^{7}Li, consistent with the LiH structure. The ^{1}H/^{7}Li heteronuclear correlation (HETCOR) spectrum (Figure 5) of NaH-LiI composite clearly shows the interactions between ^{1}H and ^{7}Li. These results also support the presence of LiH and the absence of LiI in the NaH-LiI composite.

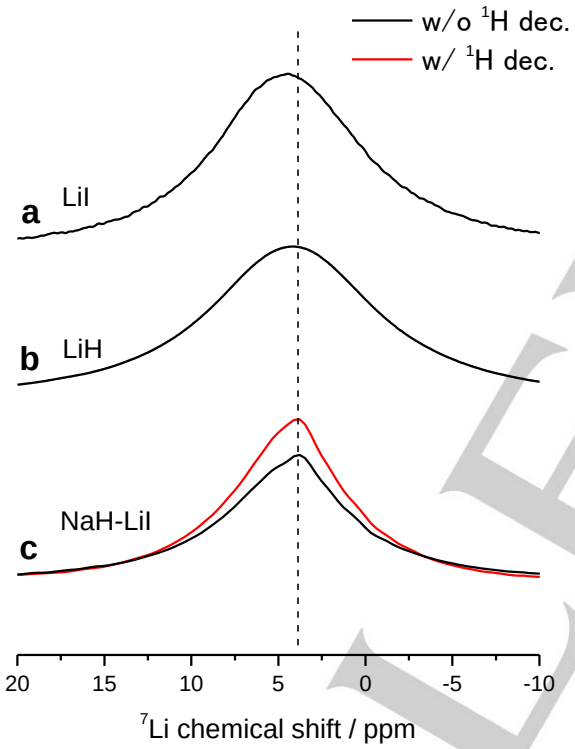

Figure 4. ^{7}Li NMR spectra of (a) LiI; (b) LiH; (c) NaH-LiI composite. The comparisons with (red) and without (black) ^{1}H decoupling are also shown. The vertical line is a guide for eye. dec. = decoupled.

In addition, ^{23}Na NMR experiments were conducted for NaI, NaH, and both the NaH-LiI and NaH-NaI composites (Figure 6). The NaI and NaH samples give discrete peaks at -2 ppm and 19 ppm, respectively, enabling us to distinguish these two structures from the ^{23}Na peak positions (Figure 6). The observed sharp lineshapes agree with the cubic symmetry in the detectable parts of these samples. The ^{1}H decoupled experiments were also performed for NaH, and both the NaH-LiI and NaH-NaI composites (Figure S7). The resolution/sensitivity improvement by ^{1}H decoupling in NaH (Figure S7a) is consistent with the proximity between ^{23}Na and ^{1}H, which is a natural consequence of the crystal structure. We can assign the peak at 19 ppm (-2 ppm) as the NaH (NaI) structure from the ^{1}H decoupled ^{23}Na spectra together with the peak position without any anbiguity. These results strongly suggest the coexistence of NaH and NaI in both the NaH-NaI and the NaH-LiI samples as confirmed by the pXRD experiments described above. However, we note that when the cubic symmetry of NaH is disrupted by NaI in a composite, the quadrupolar interactions of the ^{23}Na nuclei will be reintroduced because of the asymmetric environment around ^{23}Na. Consequently, the ^{23}Na NMR signals could have very broad lineshapes that may not be detectable.

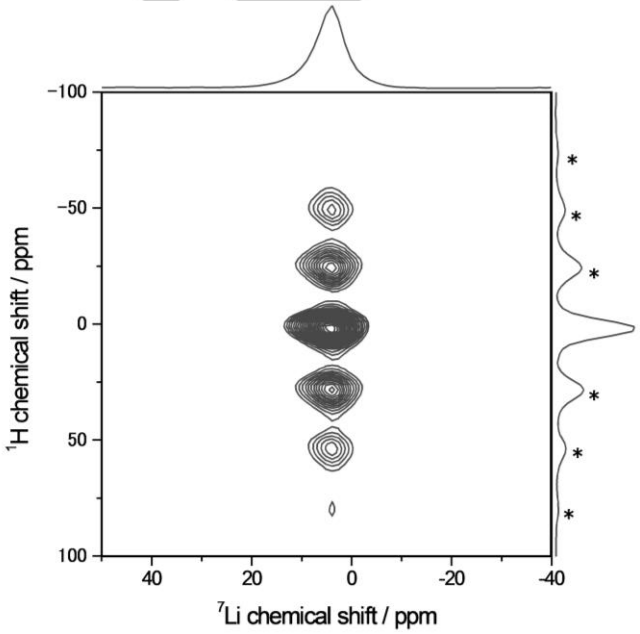

Figure 5. ^{1}H/^{7}Li HETCOR spectrum of NaH-LiI composite. The ^{1}H and ^{7}Li 1D slices at (^{1}H, ^{7}Li) = (3 ppm, 4 ppm) are also shown. The spinning sidebands signals are marked with asterisks.

We also measured the nutation curve of ^{23}Na of the NaH-NaI sample to see the effect of quadrupolar couplings (Figure S8). Although some distortion from a sine curve is observed due to the short repetition delay, both peaks behave similarly to the solution ^{23}Na samples. These experiments also confirm the cubic structure in the NaH-NaI sample through the absence of quadrupolar couplings.

Overall, the NMR data collectively indicate 1) the coexistence of NaH and NaI in both the NaH-NaI and NaH-LiI composites, 2) the absence of the LiI structure in the NaH-LiI composite, and 3) the possible formation of LiH in the NaH-LiI composite through solvothermal salt metathesis.

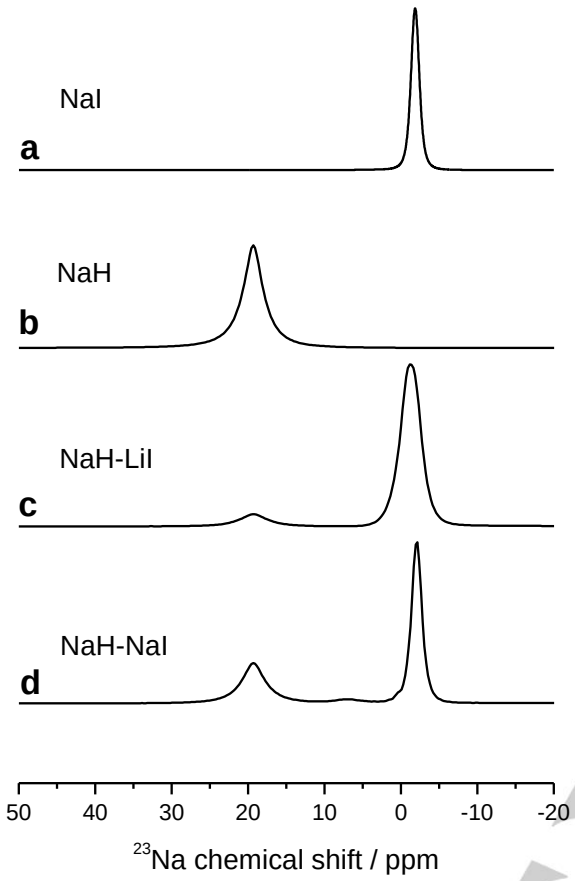

Figure 6. ^{23}Na NMR spectra of (a) NaI; (b) NaH; (c) NaH-LiI composite; (d) NaH-NaI composite.

DFT calculations on the NaH-NaI Composite

We subsequently conducted DFT calculations to investigate the origin of the hydride donor reactivity of these NaH inorganic composites and the reaction mechanisms of the decyanation using 2-phenylisobutyronitrile as a model substrate. Sodium hydride has ionic character with the cubic halite crystal structure composed of sodium metal cations and hydride anions, which make these compounds insoluble in inert organic solvents. Initially, to evaluate the intrinsic hydride donor ability of NaH, we performed DFT calculations using a *single molecule* of NaH (Figure 7a). It should be noted that DFT calculations were previously used by Bickelhaupt and Solà, to study the bonding nature of several alkali metal halides.[13] In addition, Houk reported the Hartree-Fock calculated relative stability of transition states for the reaction of NaH or LiH with carbonyl compounds, in an effort to identify the origin of π-facial selectivity.[14] Interestingly, the results of our calculations show that the barrier for hydride transfer is very low (**TS-I**, 13.3 kcal/mol), despite the commonly held belief that NaH is not capable of reducing carbonyl or cyano groups. However, the barrier for hydride transfer from the ordered crystalline sample of pure NaH is much higher (**TS-II**, 21.7 kcal/mol) than in the case of a single NaH molecule (Figure 7b).

We then sought to gain insight into how NaI provides nucleophilic hydride donor reactivity to the polymeric crystalline NaH. We built two computational models for this purpose. In one model (Model A), a 3-layer model of a NaI crystal was built first, and one of the iodine atoms on the surface was replaced with a hydrogen atom (FIgure 7c), with the intention to simulate a dispersed state of NaH. The hydride transfer reaction from this surface via **TS-III** had an energy barrier of 19.5 kcal/mol, which is lower than the barrier for the pure NaH surface by 2.2 kcal/mol. DFT calculations therefore suggest that the hydride donor reactivity of NaH is enhanced in a dispersed state. In a second model (Model B), we replaced the second layer of the NaH crystal model with a layer of NaI. With this model, we intended to derive insight into the interface of NaH and NaI crystals. Calculations indicated that the NaH cluster loses the crystalline structural integrity when a layer of NaI fragments is included, because the ionic radii of H^- and I^- are different (Figures 8 and S9). Although the computational model used here is too small compared with micron-sized NaH or the NaH-NaI composites, this computational test suggests that fragmentation is enhanced at the interface between NaH and NaI. The structural change caused by NaI has a significant impact on the nucleophilic reactivity of the *surface* NaH; thus, the barrier for hydride transfer from the surface of the NaH-NaI composite (**Ts-IV**, 16.1 kcal/mol) is lower than in the case of the ordered crystalline sample of pure NaH, resulting in a three to four orders of magnitude enhancement in rate (Figure 8).

These results indicate that *NaH is intrinsically reactive as a hydride donor to carbonyl or cyano groups, but the ordered, crystalline structure of NaH in micron-sized powders diminishes this reactivity*. However, NaI might have the effect of disrupting the crystalline nature of NaH into smaller nanometric units, thus bringing NaH closer to the reactive, isolated molecular state or the state depicted in Figure 7c. The inverse relationship between the size of the NaH crystalline units and their hydride donor reactivity, as well as the experimentally determined composition, supports the notion that the NaH-NaI inorganic composite consists of small units of NaH dispersed on NaI, and that these components interact synergistically with each other to activate the NaH.

Conclusions

In summary, we have discovered a remarkably simple protocol to prepare a new inorganic composite of NaH-NaI having intriguing nucleophilic hydride donor reactivity. A suite of characterization tools including structural analyses by pXRD, solid-state NMR spectroscopy, XPS, as well as DFT calculations allude to the recrystallization of NaI in the presence of NaH in THF. This procedure produces smaller, activated units of NaH, which are dispersed on the cubic NaI crystal phase. Synergistic cooperation between NaH and NaI at the surface of the composite is proposed to be critical for the observed hydride donor chemical reactivity to NaH. The NaH-NaI composite is

capable of unprecedented nucleophilic hydride transfer to a broad range of unsaturated substrates, such as nitriles, imines, amides, esters, and carbonyl compounds. We are working to explore further application of the present protocol to develop other kinds of nucleophilic hydride reduction with the NaH-NaI composite, as well as preparation of other new types of inorganic composites from readily available simple materials.

Experimental Section

Sample preparation of NaH-NaI and NaH-LiI composites

To a mixture of NaH and NaI or LiI in a flamed-dried 100 mL sealed tube was added 25 mL of THF in a glovebox. The reaction mixture was stirred at an external temperature of 85 °C. After cooling to room temperature, the THF was removed *in vacuo*. The vacuum-dried powder was rinsed with anhydrous pentane (3 mL × 8) in a glovebox to remove the mineral oil. This sample was used for the powder XRD, XPS, and solid-state NMR experiments. Due to the moisture sensitivity of NaH, it was always handled under N_2 in a glovebox or with Schlenk techniques under N_2 or Ar. Likewise, the sample preparation for NaH and their corresponding composites have been performed in a glovebox under N_2.

Powder X-ray diffraction

The XRD experiments were conducted using Bruker D8 Advance X-ray diffractometers, each equipped with a copper ($K_{\alpha1}$(1.54060)/$K_{\alpha2}$(1.54439) = 2) target X-ray tube set to 40 kV and 40 mA.

X-ray photoelectron spectroscopy

X-ray photoelectron spectroscopy was measured by using a Phoibos 100 spectrometer (Mg X-ray radiation source (SPECS, Germany)).

Solid-state NMR spectroscopy

All the solid-state NMR spectra were measured by a JNM-ECX400 NMR spectrometer (JEOL Ltd., Tokyo, Japan) equipped with a 4.0 mm HXMAS double resonance probe. The 90º pulse-width in the ^{1}H, ^{23}Na, ^{127}I, and ^{7}Li experiments are 2.7 μs, 3.7 μs, 4.0 μs, and 5.25 μs, respectively, which are measured with solution samples. The samples were packed into the rotor with great care to avoid air- and moisture-contamination (the samples were packed into the rotor under a N_2 atmosphere just before the NMR measurements).

FT-IR spectroscopy

FT-IR spectra were recorded on a Bruker ALPHA FTIR spectrometer in a glovebox. The Platinum ATR module was used to collect data on powder samples.

DFT calculations

A simple substrate ($PhMe_2C$-CN) was used for our DFT calculations[15] at the B3LYP/def2-TZVP or B3LYP/def2-TZVP(LANL2DZdp for I)//B3LYP/6-31G(LANL2DZ for I) level using Gaussian 09 (Rev. D.01). [15] Reported energy data contain free energy corrections at 298.15 K and 1 atm. The reaction of the substrate with one molecule of NaH was previously examined,[6a] and here, the reactions with larger models of NaH and NaH-NaI composite were studied.

Acknowledgements

Funding of SC for this work was provided by Singapore Ministry of Education (Academic Research Fund Tier 2: MOE2012-T2-1-014). HSS is supported by a start-up grant from Nanyang Technological University (NTU), the Nanyang Assistant Professorship, and the Singapore-Berkeley Research Initiative for Sustainable Energy (SinBeRISE) CREATE Program. This research program is funded by the National Research Foundation (NRF), Prime Minister's Office, Singapore under its Campus for Research Excellence and Technological Enterprise (CREATE). ZH and HSS also thank Mr. Zhang Yong Si and Prof. Mary Chan from NTU School of Chemical and Biomedical Engineering for help with DLS experiments. HH gratefully acknowledges the Nanyang Assistant Professorship and the computer resources at the High-Performance Computing Centre of NTU.

Keywords: Sodium hydride-iodide composite • X-ray diffraction • X-ray photoelectron spectroscopy • Solid-state NMR spectroscopy • Density functional calculations

[1] (a) R. E. Gawley, D. D. Hennings, *Sodium Hydride in the electronic Encyclopedia of Reagents for Organic Synthesis (e-EROS)*, D. Crich, Ed. (John Wiley & Sons, UK, 2006); (b) P. Rittmeyer, U. Wietelmann, *Hydrides in Ullmann's Encyclopedia of Industrial Chemistry* (Wiley-VCH, Weinheim, 2012); (c) S. Aldridge, A. J. Downs, *Chem. Rev.* **2001**, *101*, 3305-3366.

[2] (a) E. C. Ashby, S. A. Noding, *J. Org. Chem.* **1980**, *45*, 1041-1044; (b) P. A. A. Klusener, L. Brandsma, H. D. Verkruijsse, P. V. Schleyer, T. Friedl, R. Pi, *Angew. Chem. Int. Ed.* **1986**, *25*, 465-466; (c) R. Pi, T. Friedl, P. V. Schleyer, P. Klusener, L. Brandsma, *J. Org. Chem.* **1987**, *52*, 4299-4303; (d) T. Ohkuma, S. Hashiguchi, R. Noyori, *J. Org. Chem.* **1994**, *59*, 217-221; (e) D. Hesek, M. Lee, B. C. Noll, J. F. Fisher, S. Mobashery, *J. Org. Chem.* **2009**, *74*, 2567-2570; (f) T. Fujisawa, K. Sugimoto, H. Ohta, *J. Org. Chem.* **1976**, *41*, 1667-1668.

[3] (a) P. G. Andersson, I. J. Munslow, **2008**; (b) H. C. Brown, S. Krishnamurthy, *Tetrahedron* **1979**, *35*, 567-607.

[4] (a) X. Peng, B. M. Tong, H. Hirao, S. Chiba, *Angew. Chem. Int. Ed.* **2014**, *53*, 1959-1962; (b) K. K. Toh, A. Biswas, Y. F. Wang, Y. Y. Tan, S. Chiba, *J. Am. Chem. Soc.* **2014**, *136*, 6011-6020; (c) F. L. Zhang, Y. F. Wang, G. H. Lonca, X. Zhu, S. Chiba, *Angew. Chem. Int. Ed.* **2014**, *53*, 4390-4394; (d) A. Kaga, X. Peng, H. Hirao, S. Chiba, *Chem. Eur. J.* **2015**, *21*, 19112-19118.

[5] (a) S. K. Muduli, S. Wang, S. Chen, C. F. Ng, C. H. A. Huan, T. C. Sum, H. S. Soo, *Beilstein J. Nanotechnol.* **2014**, *5*, 517-523; (b) S. Gazi, W. K. H. Ng, R. Ganguly, A. M. P. Moeljadi, H. Hirao, H. S. Soo, *Chem. Sci.* **2015**, *6*, 7130-7142; (c) H. S. Soo, M. T. Sougrati, F. Grandjean, G. J. Long, C. J. Chang, *Inorg. Chim. Acta* **2011**, *369*, 82-91; (d) M. L. Macnaughtan, H. S. Soo, H. Frei, *J. Phys. Chem. C* **2014**, *118*, 7874-7885; (e) H. S. Soo, M. L. Macnaughtan, W. W. Weare, J. Yano, H. M. Frei, *J. Phys. Chem. C* **2011**, *115*, 24893-24905; (f) H. Shao, S. K. Muduli, P. D. Tran, H. S. Soo, *Chem. Commun.* **2016**, *52*, 2948-2951.

[6] (a) P. C. Too, G. H. Chan, Y. L. Tnay, H. Hirao, S. Chiba, **2016**, *55*, 3719-3723; (b) J. M. Mattalia, C. Marchi-Delapierre, H. Hazimeh, M. Chanon, *Arkivoc* **2006**, *2006*, 90-118; (c) F. F. Fleming, Z. Zhang, *Tetrahedron* **2005**, *61*, 747-789; (d) C. J. Sinz, S. D. Rychnovsky, **2001**, *216*, 51-92.

[7] P. A. A. Klusener, L. Brandsma, H. D. Verkruijsse, P. v. R. Schleyer, T. Friedl, R. Pi, *Angew. Chem.* **1986**, *98*, 458-459.

[8] (a) W. P. Davey, *Phys. Rev.* **1923**, *21*, 143-161; (b) C. G. Shull, E. O. Wollan, G. A. Morton, W. L. Davidson, *Phys. Rev.* **1948**, *73*, 842-847; (c) C. D. West, *Z. Kristallogr.* **1934**, *88*.

[9] Y. Kobayashi, O. J. Hernandez, T. Sakaguchi, T. Yajima, T. Roisnel, Y. Tsujimoto, M. Morita, Y. Noda, Y. Mogami, A. Kitada, et al., *Nat Mater* **2012**, *11*, 507-511.

[10] (a) C. K. Brozek, M. Dinca, *Chem. Soc. Rev.* **2014**, *43*, 5456-5467; (b) J. B. Rivest, P. K. Jain, *Chem. Soc. Rev.* **2013**, *42*, 89-96.

[11] (a) J. Kim, M. Kang, Y. Kim, J. Won, Y. Kang, *Solid State Ionics* **2005**, *176*, 579-584; (b) W. E. Morgan, J. R. Van Wazer, W. J. Stec, *J. Am. Chem. Soc.* **1973**, *95*, 751-755.
[12] V. I. Mikheeva, N. N. Mal'tseva, *J. Struct. Chem.* **1964**, *4*, 643-646.
[13] F. M. Bickelhaupt, M. Solà, C. F. Guerra, *Faraday Discuss.* **2007**, *135*, 451-468.
[14] Y. D. Wu, K. N. Houk, *J. Am. Chem. Soc.* **1987**, *109*, 906-908.
[15] (a) M. J. Frisch, G. W. Trucks, H. B. Schlegel, G. E. Scuseria, M. A. Robb, J. R. Cheeseman, G. Scalmani, V. Barone, B. Mennucci, G. A. Petersson, et al., Revision D.01 ed., Gaussian, Inc., Wallingford, CT, USA, **2009**.

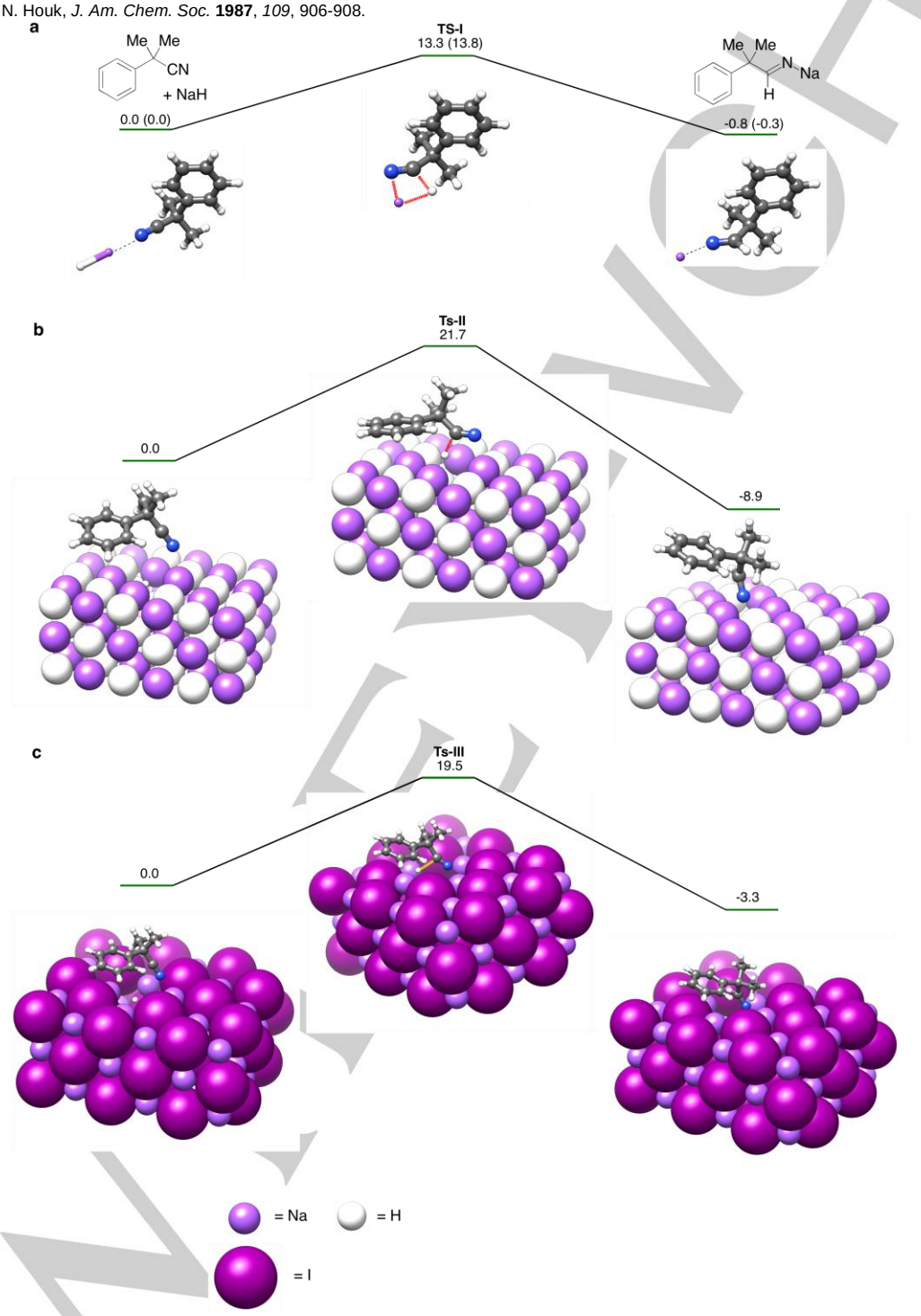

Figure 7. DFT-calculated free energy profiles for hydride reduction by NaH (in kcal/mol, B3LYP/def2-TZVP(LANL2DZdp for I)//B3LYP/6-31G(LANL2DZ for I)). (a) Reaction of 2-phenylisobutryonitrile with NaH. The values obtained at the B3LYP/def2-TZVP are also shown in parentheses for comparison. (b) Reaction with the cluster model of NaH (see Figure S9). (c) Reaction with Model A (see Figure S9). The atoms in the solid, except the hydrogen that undergoes the reaction, are represented as spheres with the following color scheme: H (white), C (grey), N (blue), Na (small violet), and I (large purple).

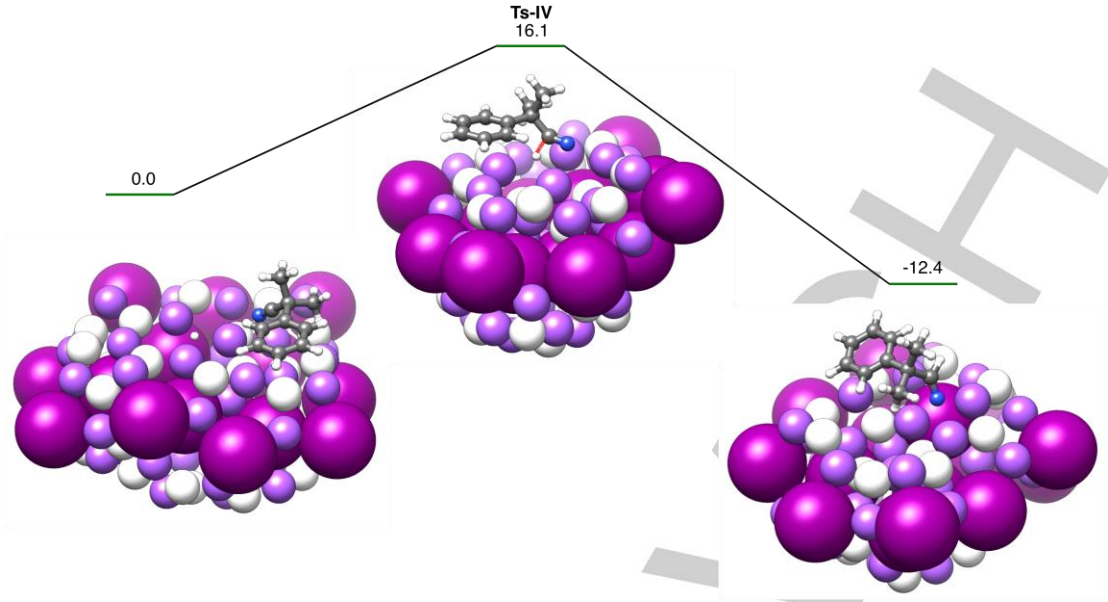

Figure 8. DFT-calculated free energy profiles for hydride reduction by NaH (in kcal/mol, B3LYP/def2-TZVP(LANL2DZdp for I)//B3LYP/6-31G(LANL2DZ for I)) in Model B (see Figure S9). The atoms in the solid, except the hydrogen that undergoes the reaction, are represented as spheres with the following color scheme: H (white), C (grey), N (blue), Na (small violet), and I (large purple).

FULL PAPER

A remarkably simple protocol is applied to activate NaH with soluble iodide ions to effect nucleophilic hydride reactivity with polar π-electrophiles. The properties of this activated NaH-NaI composite material are elucidated thoroughly using powder X-ray diffraction, X-ray photoelectron spectroscopy, solid-state NMR spectroscopy, and DFT calculations to explain the unusual reactivity of this reinvented NaH material.

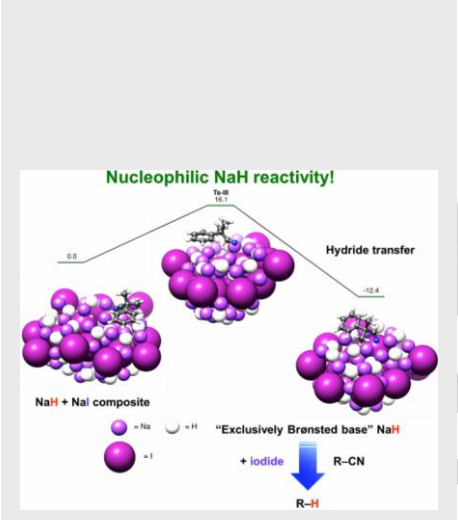

Zonghan Hong, Derek Yiren Ong, Subas Kumar Muduli, Pei Chui Tool Guo Hao Chan, Ya Lin Tnay, Shunsuke Chiba, Yusuke Nishiyama,* Hajime Hirao,* and Han Sen Soo**

Page No. – Page No.

Understanding nucleophilic hydride reactivity in NaH-NaI